Protective effects of the galectin-1 protein on in vivo and in vitro models of ocular inflammation

Caroline de Freitas Zanon,[1] Nathália Martins Sonehara,[1] Ana Paula Girol,[1,2] Cristiane Damas Gil,[3] Sonia Maria Oliani[1]

(The first two authors contributed equally to this work.)

[1]Departament of Biology, Instituto de Biociências, Letras e Ciências Exatas; São Paulo State University (UNESP), São José do Rio Preto, SP, Brazil; [2]Department of Physical and Biological Sciences, Integrated College Padre Albino Foundation (FIPA), Rua dos Estudantes, 225, Catanduva, SP, Brazil; [3]Department of Morphology and Genetics, Federal University of São Paulo (UNIFESP), São Paulo, SP, Brazil

Purpose: Galectin-1 (Gal-1) is a β-galactoside-binding protein with diverse biological activities in the pathogenesis of inflammation but has been poorly investigated in terms of ocular inflammation. In the present study, we monitored the anti-inflammatory effects of Gal-1 using the in vivo rodent model of endotoxin-induced uveitis (EIU) and in vitro assays with human RPE (ARPE-19) cells.
Methods: For this purpose, EIU was induced by subcutaneous sterile saline injection of 0.1 ml of lipopolysaccharide (LPS, 1 mg/Kg) in the rat paw, which was maintained under these conditions for 24 h. The therapeutic efficacy of recombinant Gal-1 (rGal-1) was tested in the EIU animals by intraperitoneal inoculation (3 μg/100 μl per animal) 15 min after the LPS injection. In vitro studies were performed using LPS-stimulated ARPE-19 cells (10 μg/ml) for 2, 8, 24 and 48 h, treated or not with rGal-1 (4 μg/ml) or dexamethasone (Dex, 1.0 μM).
Results: Gal-1 treatment attenuated the histopathological manifestation of EIU via the inhibition of polymorphonuclear cells (PMN) infiltration in the eye and by causing an imbalance in adhesion molecule expression and suppressing interleukin (IL)-1β, IL-6, and monocyte chemotactic protein-1 (MCP-1) productions. Immunohistochemical and western blotting analyses revealed significant upregulation of Gal-1 in the eyes induced by EIU after 24 h. In the retina, there was no difference in the Gal-1 expression, which was high in all groups, demonstrating its structural role in this region. To better understand the effects of Gal-1 in the retina, in vitro studies were performed using ARPE-19 cells. Ultrastructural immunocytochemical analyses showed decreased levels of endogenous Gal-1 in LPS-stimulated cells (24 h), while Dex treatment upregulated this protein. The protective effects of rGal-1 on LPS-stimulated cells were associated with the significant reduction of the release of cytokines (IL-8 and IL-6), similar to Dex treatment. Furthermore, rGal-1 and Dex inhibited cyclooxygenase-2 (COX-2) expression in LPS-stimulated cells, as shown by immunofluorescence.
Conclusions: Overall, this study identified potential roles for Gal-1 in ocular inflammation, especially uveitis, and may lead to future therapeutic approaches.

Endotoxin-induced uveitis (EIU) is a widely accepted animal model for improving our understanding of ocular inflammation [1-3]. Although EIU is generally considered to be an inflammation of the anterior uvea, changes in the posterior segment involving the vitreous and retina may also occur [3-6]. Lipopolysaccharide (LPS) is an exogenous bacterial toxin used in the induction of EIU because it binds to toll-like receptor 4 (TLR4) [7] and stimulates the synthesis and the release of proinflammatory chemical mediators, such as nitric oxide (NO) [2,8], platelet-activating factor (PAF),

tumor necrosis factor-α (TNF-α), interleukin-1β (IL-1β), IL-6, monocyte chemotactic protein-1 (MCP-1) [9], and other cytokines [10,11]. This increased expression of inflammatory mediators exacerbates the development of uveitis by breaking down the blood–ocular barrier, which leads to edema formation and contributes to leukocyte influx [10,12,13].

The pharmacological treatments for uveitis include corticosteroids and chemotherapeutic agents, but the side effects of these drugs, such as increased ocular pressure and cytotoxicity, limit their use and highlight the need for new therapeutic approaches [3,14-16]. Among the available anti-inflammatory mediators, the Galectin-1 (Gal-1) protein acts in particular to limit the development of an acute inflammatory process [17-21].

Galectins are lectin family members defined by their affinity for β-galactoside carbohydrates and their shared

Correspondence to: Sonia Maria Oliani. Departament of Biology, Instituto de Biociências, Letras e Ciências Exatas; São Paulo State University (UNESP), Rua Cristóvão Colombo, 2265, Jardim Nazareth, 15054-000, São José do Rio Preto, SP, Brazil; Phone +55 17 3221-2380; FAX: +55 17 3221-2390; email: smoliani@ibilce.unesp.br

consensus amino acid sequences in the carbohydrate recognition domain (CRD). They are widely expressed in various tissues and organs, showing the highest expression in the immune system [22,23]. Gal-1 is a prototypic member of this family, with anti-inflammatory properties described in several models of chronic and autoimmune inflammation, including autoimmune encephalomyelitis [24], arthritis [25], uveitis [26], hepatitis [19], and diabetes [27]. This protein participates in the interaction between the cell surface and extracellular matrix through binding to glycoconjugated proteins [28] and inhibits the rolling and extravasation of polymorphonuclear cells (PMNs) into sites of inflammation [21].

Although the anti-inflammatory activities of Gal-1 have been explored in several in vivo and in vitro investigations [29-33], the exogenous role of this protein in ocular inflammatory processes has been poorly elucidated. Given the common side effects of the current therapies used to treat uveitis [14-16], we evaluated the effects of endogenous and exogenous Gal-1 protein in rodent ocular tissues in EIU and in an in vitro LPS-inflamed RPE human cell system. These analyses shed light on the genesis of the role of Gal-1 in ocular inflammation, especially uveitis, and indicate its potential for use as a therapeutic approach.

METHODS

In vivo studies:

Animals—Male Wistar rats (*Rattus norvegicus*) weighing 150–200 g were randomly distributed into four groups (n = 10 per group). The animals were housed under a 12h:12h light-dark cycle and were allowed access to food and water ad libitum. All of the experiments were conducted in compliance with the Association for Research in Vision and Ophthalmology Statement for the Use of Animals in Ophthalmic and Vision Research. The study was approved by the Ethics Committee on Animal Experimentation of São José do Rio Preto Medical School (No. 0467/2009).

Induction of EIU and rGal-1 treatment—To induce EIU development, the rats were inoculated in the right paw with 1 mg/kg of LPS from *Escherichia coli* serotype O127:B8 (Sigma-Aldrich, St Louis, MO); Sigma Chemical, Poole, UK) diluted in 0.1 ml of sterile saline [6]. The animals were then maintained under these conditions for 24 h. The therapeutic efficacy of a recombinant Gal-1 (rGal-1) protein was tested in the EIU animals for 24 h. The rats were inoculated with LPS as described above, and after 15 min, they were treated intraperitoneally (i.p.) with rGal-1 (PeproTech EC Ltd., London, UK) at a concentration of 3 µg/100 µl per animal [34], then euthanized after 24 h. No manipulated animals were used

as control. The animals were anesthetized with isoflurane (1%) before all experimental treatments and were euthanized through an overdose of the anesthetic.

Histopathological analysis—After collecting aqueous humor (AqH), the right eyes of the control and experimental rats (n = 5 per group) were fixed in a 4% paraformaldehyde, 0.5% glutaraldehyde solution (1:1) in sodium cacodylate buffer 0.1 M (pH 7.4) for 24 h at 4 °C and then bisected. A portion of these eye fragments were dehydrated using graded methanol solutions and embedded in LR Gold resin (Sigma-Aldrich) [35] for histopathology, while the other portion was embedded in paraffin for immunohistochemistry. Quantitative analysis of neutrophils was performed in 1 µm tissue sections from the anterior and posterior eye segments in a blind manner, with counting performed using a high-power objective (40X) on an Axioskop 2-Mot Plus Zeiss microscope (Carl Zeiss, Jena, Germany). The number of neutrophils was quantified in three semiserial sections per animal with a 30 µm distance between each section, and the values are reported as the mean (± standard error of the mean [SEM]) number of cells/mm^2.

Quantitative analysis of leukocytes in AqH and blood—AqH was collected from the right eyes of the rats (n = 5 per group) by puncturing the anterior chamber with a 28-gauge needle, and a 10 µl aliquot of AqH was stained with Turk solution (90 µl). Blood was collected through cardiac puncture (n = 5 per group), and a 10 µl sample of whole blood was diluted in 190 µl of Turk solution. Neutrophils and monocytes/macrophages (mono-Møs) were quantified in a Neubauer chamber (Laboroptik; Friedrichsdorf, Germany). Data are reported as the mean ± SEM of the average number of cells x 10^5/ml in the AqH samples and the number of cells x 10^3/ml in the blood samples.

Blood flow cytometry—Whole blood was collected in EDTA (100 mg/ml) via cardiac puncture (n = 5 per group). Aliquots (10 µl) of animal blood were incubated with 1 µl of a monoclonal antibody against L-selectin conjugated with phycoerythrin (PE; anti-rat CD62L; BD Pharmigen, San Diego, CA) and β2-integrin conjugated with fluorescein isothiocyanate (FITC; anti-rat CD11b; BD PharMingen) diluted 1:10 in PBS (1X; 120 mM NaCl, 20 mM KCl, 10 mM NaPO$_4$, 5 mM KPO$_4$, pH 7.4) for 20 min at 4 °C in the dark. Immediately after incubation, 180 µl of Guava Lysing Solution/Fixative (EMD Millipore, Billerica, MA) was added to lyse and fix the cells for 20 min at 37 °C. The cells were analyzed using a Guava EasyCyte flow cytometer (Millipore Corporation), and leukocytes were gated according to the side and forward scatter parameters. Data were obtained from 10,000 cells (only morphologically viable cells were

considered in the analysis) to determine the percentages (%) of CD62L and CD11b-positive cells.

Immunohistochemistry—To study the specific localization of Gal-1, 5 μm sections of paraffin-embedded eyes were employed. Following an Ag retrieval step using citrate buffer (pH 6), endogenous peroxide activity was blocked, and the sections were incubated overnight at 4 °C with a primary rabbit polyclonal anti-Gal-1 antibody (Ab; 1:200; Zymed Laboratories, Cambridge, UK) diluted in 1% bovine serum albumin (BSA). After washing, the sections were incubated with a biotinylated secondary Ab (KIT Histostain-SP; Invitrogen, Frederick, MD). Positive staining was detected using a peroxidase-conjugated streptavidin complex, and the color was developed using 3,3′-diaminobenzidine (DAB) as a substrate (Invitrogen). The sections were counterstained with hematoxylin. For densitometric analyses, three slides from each animal (n = 5 per group) were used, and 20 points were analyzed in three fields in the cornea, ciliary processes, and retina (plexiform layers, ganglion cells, and PE). In addition, 10 points were marked on the iris and retina to obtain an average related to the intensity of immunoreactivity. The values were obtained as arbitrary units (a.u.) using the Axio-Vision software (Carl Zeiss).

Western blotting analysis—To detect total amounts of Gal-1 and adhesion molecules (CD62L and CD11b), the left eyes of rats (n = 5 per group) subjected to different experimental conditions were macerated in liquid nitrogen and lysed on ice for 15 min with 1 ml of a solution containing one complete mini EDTA-free protease inhibitor mixture tablet (Roche Applied Science, Mannheim, Germany), 50 mM Tris-HCl, 150 mM NaCl, and 1% Triton-X (pH 7.4). The samples were then transferred to microtubes and centrifuged at 10,000 ×g for 20 min at 4 °C. The protein concentration in the eye supernatants was measured using the BCA™ Protein Assay Kit (Pierce Biotechnology, Rockford, IL). All protein samples were stored in aliquots at -80 °C until analysis. Equal amounts of rat samples (31.5 μg) and molecular weight markers were separated by electrophoresis in 12% polyacrylamide gel according to the Mini-PROTEAN Tetra Cell (Bio-Rad, Hercules, CA) protocol and transferred to nitrocellulose membranes (Hi-Bond C, Amersham Biosciences, Little Chalfont, UK). Target proteins were detected in rat samples using the rabbit polyclonal anti-Gal-1 AB (3 μg/ml; Zymed Laboratories), anti-CD62L (1:200), anti-CD11b (1:200; Santa Cruz Biotechnology, Santa Cruz, CA), anti-β-actin (1:500; BioLegend, San Diego, CA) and anti-glyceraldehyde 3-phosphate dehydrogenase (GAPDH; 1:5000; Sigma-Aldrich). The Western Breeze Immunodetection Kit (Invitrogen) was used for the chromogenic detection of Gal-1 and β-actin bands.

Adhesion molecules and GAPDH were detected using an enhanced Supersignal West Pico Chemiluminescent Substrate Kit (Thermo Fisher Scientific) and film was developed in dark room. Protein densitometry was performed using the software ImageJ 1.440 (HIH, Bethesda, MD) to determine relative expression (a.u.) of Gal-1/β-actin.

In vitro studies:

Cell culture and treatment protocols—ARPE-19 cells were purchased from the American Type Culture Collection (ATCC, Manassas, VA; short tandem repeat analysis [STR] was showed in Appendix 1) and grown in a mixture (1:1) of Dulbecco's Modified Eagle's Medium (DMEM):Nutrient F-12 Ham (Sigma-Aldrich) [36] supplemented with 10% fetal bovine serum (FBS), 200 mM L-glutamine, 0.1 mg/ml streptomycin, and 100 U/ml penicillin (Invitrogen). To determine the optimal length of treatment with rGal-1 (PeproTech EC Ltd.), ARPE-19 cells were initially cultivated in complete medium, as described previously, and incubated with 10 μg/ml LPS (Sigma-Aldrich) for 2, 8, 24, or 48 h. The tested LPS concentration was chosen based on a study that used the same cell line [3]. To evaluate the anti-inflammatory effect of Gal-1, concentrations of 0.04, 0.4, and 4.0 μg/ml of rGal-1 were tested in the LPS-stimulated cells [18,30]. As positive control for the anti-inflammatory effects on LPS-stimulated cells, we used the glucocorticoid Dex (Sigma-Aldrich) at a concentration of 1.0 μM [37] (five independent experiments per group). Subsequently, the supernatants were collected to measure the levels of the proinflammatory cytokines IL-8 and IL-6. The results revealed that the 4.0 μg/ml concentration of rGal-1 was the most effective in significantly reducing the levels of both cytokines compared with LPS-stimulated cells. After determining the best treatment protocol, we established the experimental design. Cells were subjected to the following experimental conditions: growth in complete medium (control), activation by LPS (10 μg/ml) without treatment or treatment with 4.0 μg/ml of rGal-1 (LPS/rGal-1) or 1.0 μM of Dex (LPS/Dex). The cytotoxic effect of rGal-1 relating to the proliferation and viability of ARPE-19 cells was investigated in all experimental groups at 2, 8, 24, and 48 h. The cells were trypsinized and quantified using a Countess Automated Cell Counter (Invitrogen). The results revealed no significant differences in the rate of cell proliferation or cell viability among the experimental groups compared with their respective controls. Cellular morphology was evaluated using an inverted microscope (CKX41; Olympus). The experimental procedures were conducted in accordance with the rules of the Research Ethics Committee of the Institute of

Bioscience, Letters and Exact Science, IBILCE/UNESP, São José do Rio Preto (nº 041/11).

Fixation, processing, and embedding for transmission electron microscopy—ARPE-19 cells were fixed in a 4% paraformaldehyde, 0.5% glutaraldehyde solution (1:1) in sodium cacodylate buffer 0.1 M (pH 7.4) for 24 h at 4 °C. The cells were subsequently dehydrated through a methanol series and embedded in LR Gold resin (Sigma-Aldrich).

Postembedding immunogold labeling—To detect the localization of the endogenous Gal-1 protein, ultrathin sections (70 nm) of ARPE cells were sequentially incubated with the following reagents at room temperature: i) distilled water; ii) PBS containing 1% egg albumin (1% PBEA) for 10 min; iii) 5% PBEA; iv) rabbit polyclonal anti-Gal-1 Ab (1:100; Zymed Laboratories) for 2 h, with normal rabbit serum as a control (1:100); and v) 1% PBEA containing 0.01% Tween-20 in three washes (5 min each). To detect Gal-1, a goat anti-rabbit IgG Ab (1:50 in 1% PBEA) conjugated with 15 nm colloidal gold (British Biocell, Cardiff, UK) was applied. After 1 h, the sections were washed thoroughly in 1% PBEA and then in distilled water. These sections were stained with uranyl acetate and lead citrate and then examined using a ZEISS Leo 906 electron microscope (Carl Zeiss). Randomly photographed sections of ARPE cells were used for immunocytochemical analysis. The area of the cell compartment was determined with AxioVision software on an Axioskop 2-Mot Plus Zeiss microscope. The density of immunogold particles (number of gold particles per μm^2) was calculated and expressed for each cell compartment. Values are reported as the mean ± SEM of 10 electron micrographs analyzed per group.

Immunofluorescence analysis—To detect cyclooxygenase-2 (COX-2), ARPE-19 cells were grown on coverslips, fixed in 4% paraformaldehyde for 24 h, washed in PBS and Tween-20 (0.4%), blocked with 1% BSA, diluted in 3% normal goat serum, and incubated with a polyclonal rabbit anti–COX-2 Ab (Abcam, Cambridge, UK; 1:200 in normal goat serum 1.5%). After washing, the cells were incubated with goat anti-rabbit Ab conjugated with FITC (Serotec, Oxford, UK; 1:100 in normal goat serum 1.5%) for 1 h. The slides were mounted with a solution containing glycerol and PBS (1:1). Normal goat serum was used in the reaction control. The cells were analyzed using a filter with a wavelength of 546 nm on an Axioskop 2-Mot Plus Zeiss microscope, and the levels of the enzyme were quantified via densitometry.

Procedures in vivo and in vitro:

Quantitative analysis of chemical mediators in the supernatants of ocular tissues and ARPE-19 cells—The levels of IL-1β, IL-6, and MCP-1, which are chemical mediators generally linked to EIU [9,12], were analyzed in the supernatants of the ocular tissues obtained following maceration (n = 5 per group). However, the cytokines IL-8, IL-6, and MCP-1 were the chemical mediators released in the largest quantities by ARPE-19 cells following LPS activation for 24 h [3,38]; therefore, they were analyzed in the cell supernatants under all experimental conditions. The supernatants of the ocular tissues, obtained following maceration of eyes (n = 5 per group), were analyzed using the MILLIPLEX RAT Cytokine/Chemokine Magnetic Bead panel (catalog number RECYTMAG-65K; Millipore Corporation, Billerica, MA). The kit can detect IL-1β, IL-6, and MCP-1 cytokines simultaneously in a single sample. The samples were brought to room temperature and added in duplicate to 96-well filter-bottom plates. Antibody-coated detection beads were added to the wells and incubated with agitation on plate shaker for 1 hour at room temperature (20-25 °C). Without aspirated after incubation, the beads were further incubated with streptavidin-phycoerythrin for 30 min. Then 125 μl of sheath fluid were added to each well, and the samples were analyzed using Luminex laser-based fluorescent analytical test instrumentation (MAGPIX, Austin, TX). Cytokine concentrations were determined from standard curves prepared on each plate and expressed as picogram per milliliter (pg/ml).

For the in vitro assays, IL-6, IL-8 and MCP-1 levels in the ARPE-19 cell supernatants were detected using a commercially available Human Quantikine ELISA Kits (R&D Systems, Minneapolis, MN) and according to the manufacturer's instructions. Briefly, 100 μl of each of the standards, controls, and samples were loaded onto a 96-well polystyrene microplates containing 100 μl assay diluent in duplicate. After incubation for 2 h at room temperature, the microplates were washed 4X. Then, 200 μl of specific human IL-6, IL-8 or MCP-1 conjugate solutions were added to each well for 2 h at room temperature, washed 4X and 200 μl of a substrate solution were added. After 20 min of incubation, 50 μl of the stop solution was added, and the optical density was read at 450 nm using a microplate reader (Molecular Devices, Sunnyvale, CA) with a correction wavelength of 540 nm. The cytokines concentration of each sample was calculated from the standard curve..

Statistical analysis—Data were presented as mean ± SEM. A statistical analysis was performed with GraphPad Prism (GraphPad Software Inc., version 5.0). The results were previously subjected to descriptive analysis and determination

of normality using the Kolmogorov–Smirnov test. For samples with a normal distribution, we applied analysis of variance (ANOVA), followed by a Bonferroni correction for multiple comparisons or t tests for unpaired samples. The Kruskal–Wallis test followed by Dunn's test was used for samples with a non-normal distribution. A p-value less than 0.05 was considered statistically significant.

RESULTS

rGal-1 attenuates ocular inflammation: In the eyes of control rats, an absence of transmigrated neutrophils was observed in the anterior (Figure 1A-B) and posterior (Figure 1C) segments. In contrast, 24 h after intraocular injection of LPS, an influx of neutrophils was detected in the anterior ocular segment ($p < 0.001$), followed by transmigration to the AqH, as well as in the stroma of the iris, ciliary processes (Figure 1D), and limbus (Figure 1E). In addition, the posterior segment of the eye presented neutrophils that transmigrated to the vitreous and retina ($p < 0.01$), especially in the inner plexiform layer (Figure 1F). Treatment with rGal-1 induced a decrease in the number of transmigrated neutrophils in both the anterior (Figure 1J; $p < 0.01$) and the posterior (Figure 1K, $p < 0.01$) segments compared with the LPS group.

rGal-1 inhibits neutrophil influx and enhances the recruitment of mononuclear phagocytic cells in the AqH and blood in EIU: At 24 h after LPS injection, an intense inflammatory response characterized by a significant increase in the number of neutrophils in the AqH (Figure 2A; $p < 0.01$) and blood (Figure 2B; $p < 0.001$) was detected compared to the control group.

The effect of pharmacological treatment with rGal-1 on the recruitment of leukocytes was also evaluated, revealing a significant decrease in the number of neutrophils in the AqH (Figure 2A; $p < 0.05$) and blood (Figure 2B; $p < 0.01$) compared with the untreated LPS group. Quantification of mononuclear phagocytic cells showed an exacerbated number of these cells following the treatment with rGal-1 in the AqH (Figure 2C; $p < 0.001$) and blood (Figure 2D; $p < 0.001$) compared to the LPS and control groups.

Gal-1 modulated adhesion molecules L-selectin and β2-integrin: The expression of adhesion molecules on leukocytes in the peripheral blood was investigated under the different experimental conditions via flow cytometry. The analysis of dot plot graphs demonstrated a high incidence of CD62L-positive cells (Figure 3B; $p < 0.05$) compared to the control groups (Figure 3A). However, the LPS + rGal-1 group showed a high incidence of CD62L/CD11b-positive and CD11b-positive cells (Figure 3C; $p < 0.01$) and a low percentage of CD62L-positive cells ($p < 0.001$) compared

to the LPS group. Analysis of the percentages of CD62L-, CD11b-, and CD62L/CD11b-positive cells confirmed this observation (Figure 3D-F). Similarly, immunoblot analysis of pooled extracts of rat eyes (n = 5 animals/group) revealed high levels of both adhesion molecules in the LPS + rGal-1 group compared to the untreated LPS group at 24 h (Figure 3G).

*In vivo and in vitro administration of rGal-1 modulates proinflammatory mediators release during ocular inflam*mation: As expected, the levels of IL-1β, IL-6, and MCP-1 increased significantly in the eyes 24 h after LPS injection (Figure 4A-C; $p < 0.001$, $p < 0.05$, and $p < 0.01$, respectively). Administration of rGal-1 decreased the levels of IL-1β ($p < 0.05$) and IL-6 ($p < 0.05$) after 24 h compared with the untreated animals. In addition, the administration of rGal-1 induced a significant increase of chemokine MCP-1 compared to the control group (Figure 4C; $p < 0.05$).

Considering that in vivo LPS-induced ocular inflammation enhanced neutrophil infiltration and cytokine secretion, which were reversed by rGal-1 treatment, we investigated the role of Gal-1 in the secretion of chemotactic cytokines and the cellular localization of COX-2 in LPS-stimulated ARPE-19 cells after 24 h. Because LPS induces RPE cells to secrete high levels of IL-8 and IL-6, we checked these mediators in the cell supernatants. We observed a significant increase in the levels of IL-8 ($p < 0.001$) and IL-6 ($p < 0.01$) in the LPS-stimulated cells relative to the control (Figure 4D,E). The rGal-1 (4.0 μg/ml) and Dex treatments markedly reduced the levels of both cytokines ($p < 0.001$ and $p < 0.01$, respectively). For MCP-1, there was no difference in the LPS group relative to the control (Figure 4F). However, treatment with rGal-1 (4.0 μg/ml) increased release the levels of this chemokine compared to the control and to the LPS (Figure 4F; $p < 0.0.01$ and $p < 0.05$).

In addition, LPS-stimulated ARPE-19 cells revealed intense cytoplasmic positivity of COX-2 compared to control cells (Figure 4G; $p < 0.001$), while Dex and rGal-1 treatments efficiently reduced this cytoplasmic immunoreactivity (Figure 4G; $p < 0.001$). Densitometry analysis confirmed these observations (Figure 4H).

Endogenous Gal-1 expression is modulated in ocular tissues and ARPE-19 cells during inflammation: Immunohistochemistry analysis demonstrated the presence of Gal-1 expression in the epithelia of the cornea, ciliary processes, and iris (Figure 5A-C). There was an increase in Gal-1 expression in these regions 24 h after LPS injection (Figure 5D-F; $p < 0.01$, $p < 0.01$, and $p < 0.001$, respectively) compared with the control tissues. However, we observed reduced expression of Gal-1 in the cornea and ciliary processes in the animals
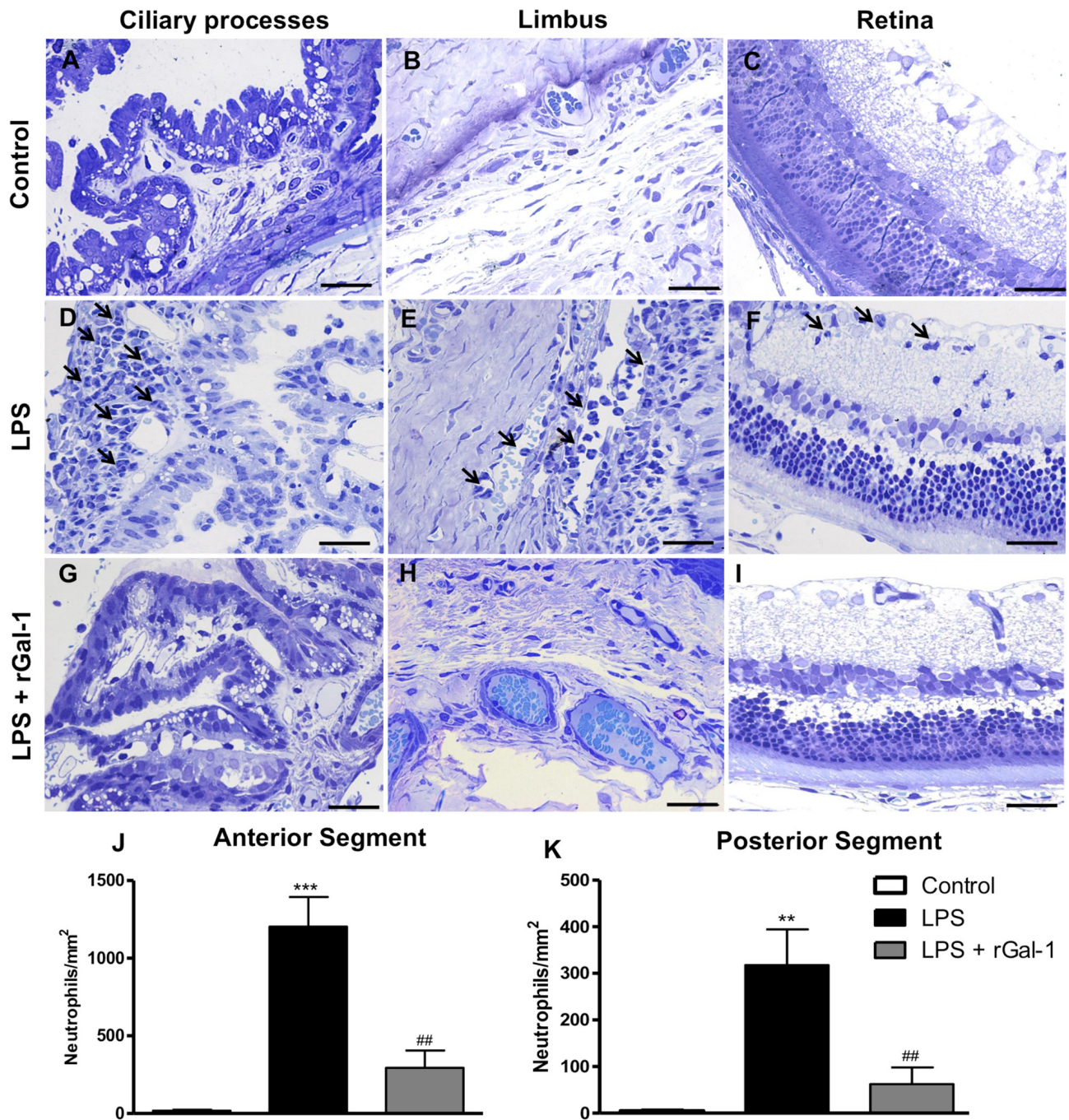
Figure 1. rGal-1 alleviated inflammation in EIU experimental model in rats. **A–C**: Absence of neutrophils in control ocular tissues. **D–F**: Influx of neutrophils (arrows) in the ciliary processes, limbus, and retina 24 h after the induction of uveitis by lipopolysaccharide (LPS). **G–I**: After treatment with recombinant galectin-1 (rGal-1). Sections: 1 μm. Scale bars, 20 μm. **J**, **K**: Quantitative analysis of neutrophils in the anterior (**J**) and posterior segments (**K**) of the eye. Values represented mean ± SEM of the number of neutrophils/mm^2 (n = 5) ***p<0.001, **p<0.01 versus control; ##p<0.01 versus LPS.
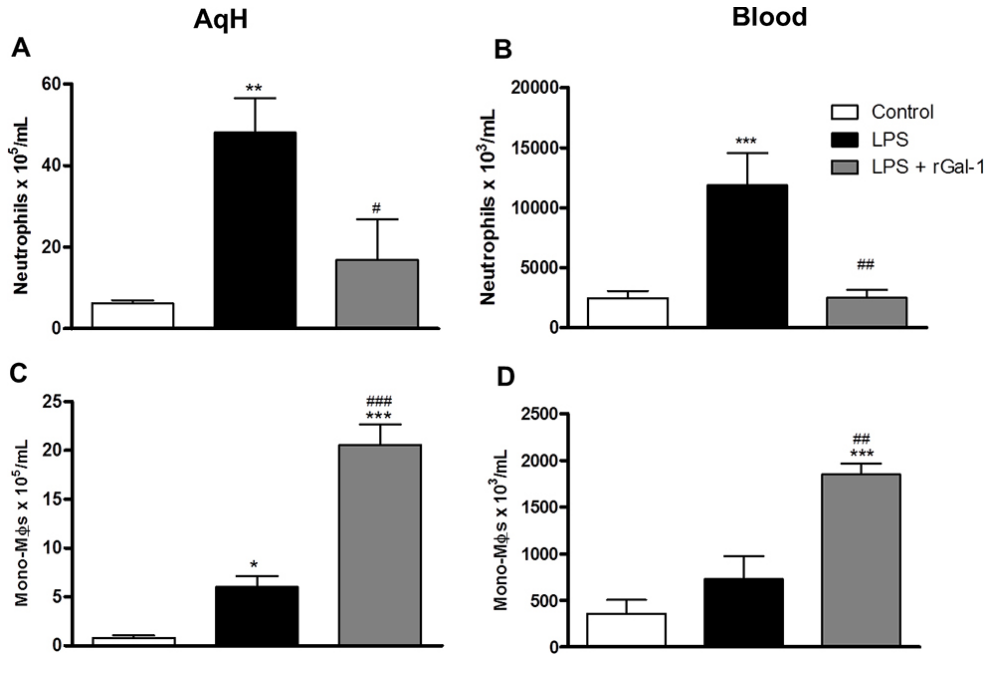
Figure 2. Quantitative analysis of neutrophils and mononuclear phagocytic cells in aqueous humor and blood. **A**, **C**: Aqueous humor [AqH]. **B**, **D**: Blood. Mononuclear phagocytic cells [Mono-Møs]. Data represents the mean ± SEM of the number of cells x 10^5 per ml (AqH) and x 10^3 per ml (blood; n = 5); *$p<0.05$, **$p<0.01$, ***$p<0.001$ versus control; #$p<0.05$, ##$p<0.01$, ###$p<0.001$ versus LPS.
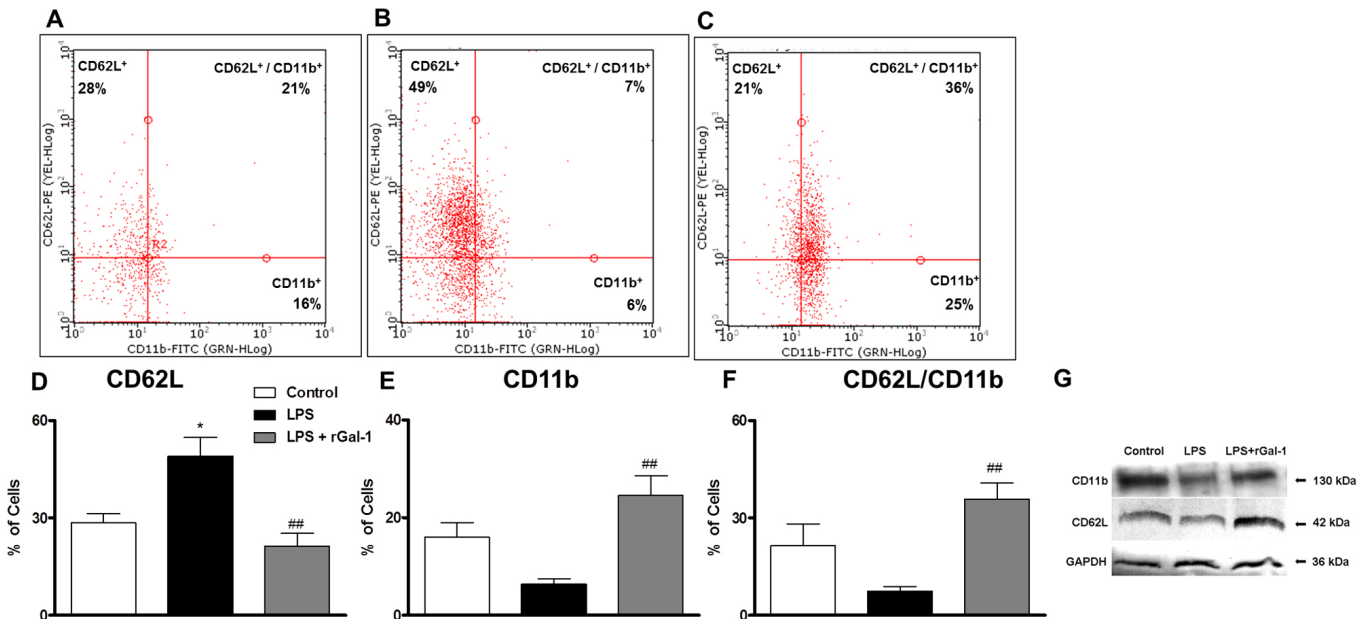

Figure 3. rGal-1 modulates L-selectin and β2-integrin. Peripheral leukocytes were labeled with antibodies specific for the surface adhesion molecules CD62L (conjugated with PE) and CD11b (conjugated with fluorescein isothiocyanate [FITC]). **A-C**: Representative dot plots of cells (each point represents a cell) immunostained for adhesion molecules. **A**: Control, **B**: LPS, **C**: LPS + recombinant galectin-1 (rGal-1), **D**: percentages of CD62L-positive cells, **E**: CD11b-positive cells, and **F**: CD62L/CD11b-positive cells. Data represent the median ± SEM of percentage of cells. *$p<0.05$, versus control; ##$p<0.01$ versus LPS. **G**: Representative immunoblot demonstrates the levels of CD11b and CD62L in the pooled extracts of rat eyes (n = 5 animals/group) from the control, LPS, and LPS + rGal-1 groups at 24 h (data illustrate one representative of two independent experiments). Glyceraldehyde 3-phosphate dehydrogenase (GAPDH) was used as loading control.
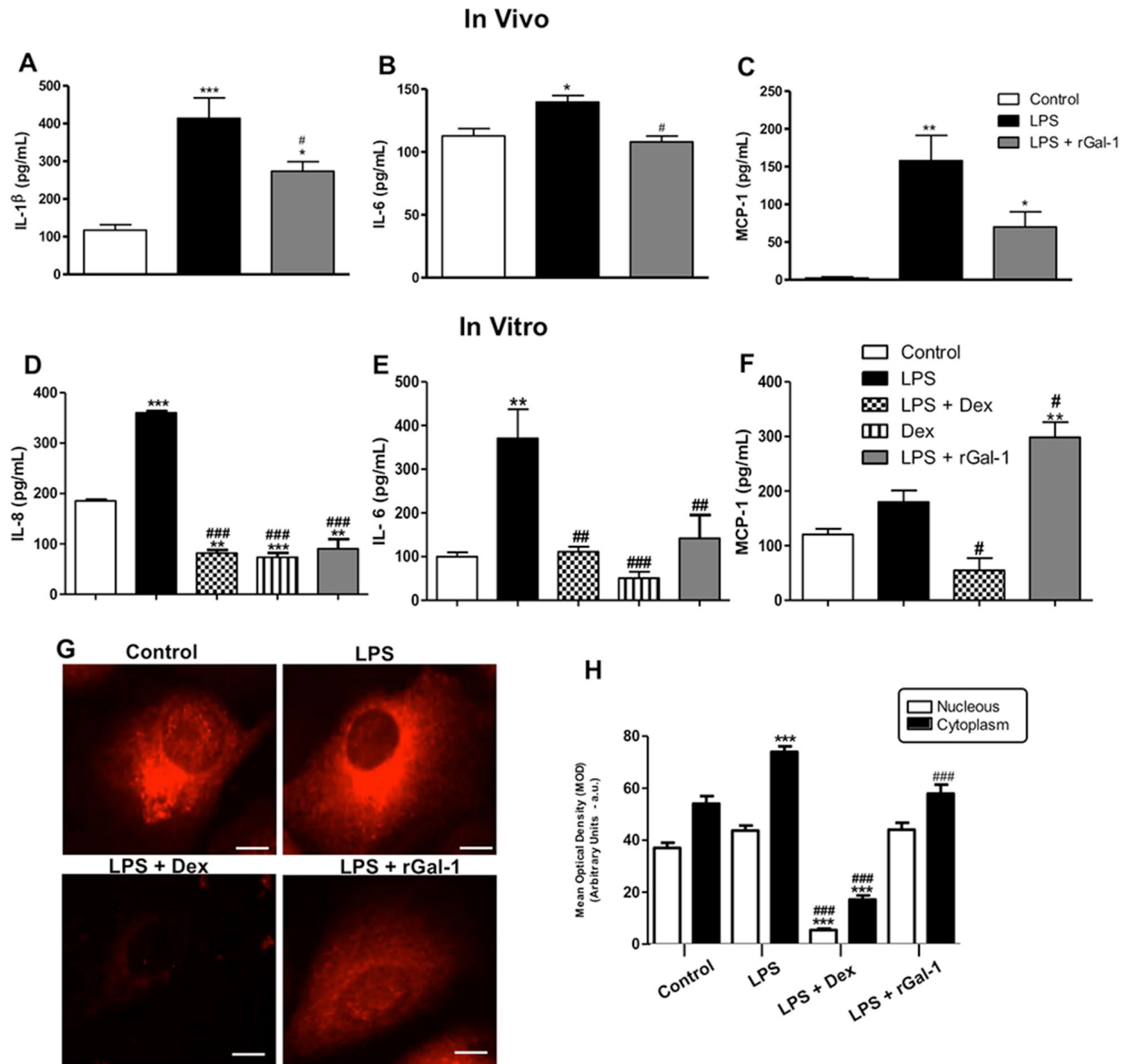
Figure 4. **In vivo and in vitro administration of rGal-1 modulates proinflammatory mediators release during ocular inflammation:** IL-1β (**A**), IL-6 (**B**), and MCP-1 (**C**) in ocular tissues (in vivo). Interleukin-8 (IL-8) (**D**), IL-6 (**E**), and monocyte chemotactic protein-1 (MCP-1; **F**) in ARPE-19 cells (in vitro). Data are expressed as the mean ± SEM (pg/ml) from the eye homogenates (n = 5) or cell supernatants. * $p < 0.05$, ** $p < 0.01$, *** $p < 0.001$ versus control; #$p < 0.05$, ##$p < 0.01$, ###$p < 0.001$ versus lipopolysaccharide (LPS) or LPS-stimulated cells. (**G**) Cyclooxygenase-2 (COX-2) immunofluorescence in ARPE-19 cells showed decreased COX-2 immunoreactivity in the cytoplasm after recombinant galectin-1 (rGal-1) treatment in LPS-stimulated cells after 24 h. Bars: 10 µm. **H**: Densitometric analysis of COX-2. The data are presented as the mean ± SEM of the densitometric index (arbitrary units [a.u.]) of cells from three independent experiments. ***$p < 0.001$ versus control; ###$p < 0.001$ versus LPS.
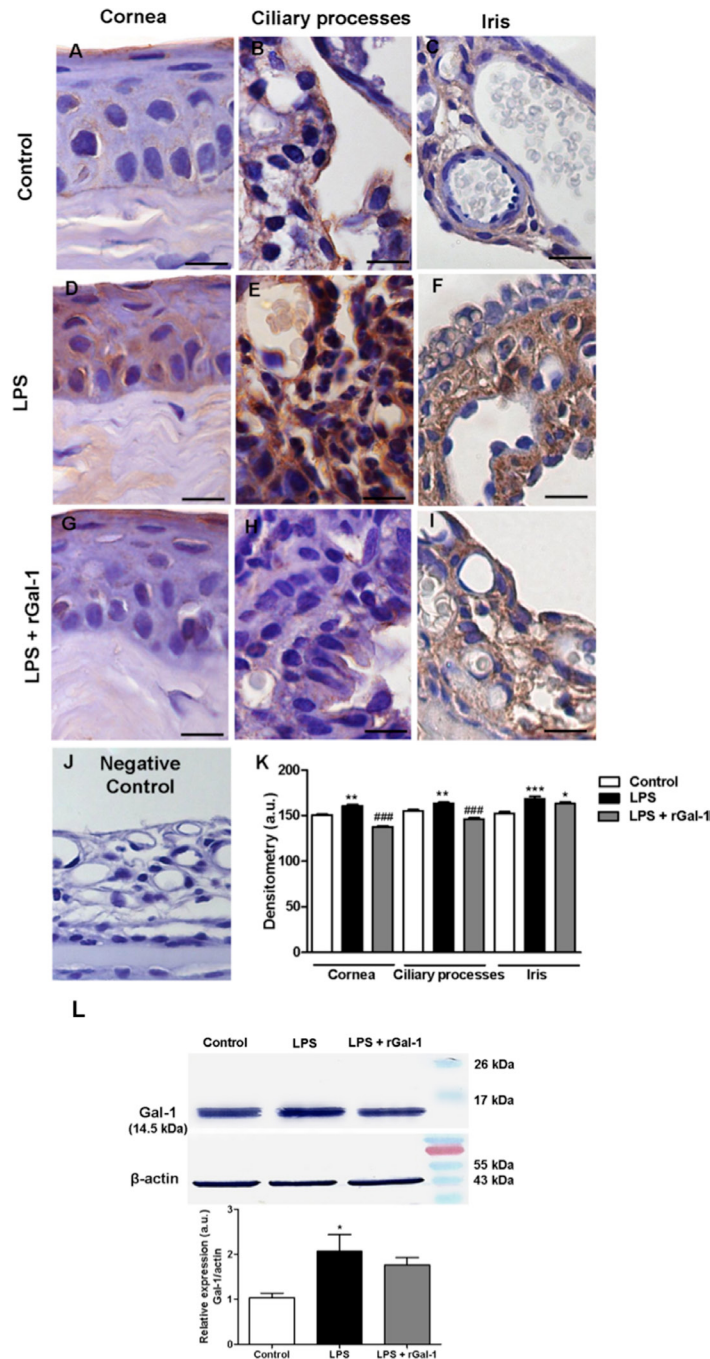
Figure 5. Gal-1 expression in the anterior eye segment and eye supernatants. **A**: Galectin-1 (Gal-1) immunoreactivity in the epithelial cells of the cornea, **B**: ciliary body, and **C**: iris in the control group. **D-F**: Lipopolysaccharide (LPS) group with intense immunostaining in the epithelium. **G-I**: LPS + recombinant Gal-1 (rGal-1) group showing diminished Gal-1 expression in epithelial cells. **J**: No immunostaining was detected in the negative control section (without primary antibody). Counterstain: hematoxylin. Bars: 20 µm. **K**: Densitometric analysis of Gal-1 expression in epithelial cells. **L**: Representative western blot. Equal loading was confirmed using anti–β-actin. Immunoreactive protein bands were semiquantified via densitometry and expressed in arbitrary units (a.u.) relative to β-actin. Values (a.u.) are presented as the mean ± SEM of sections analyzed (n = 5). *p<0.05, **p<0.01, ***p<0.001 versus control; ###p<0.001 versus LPS.
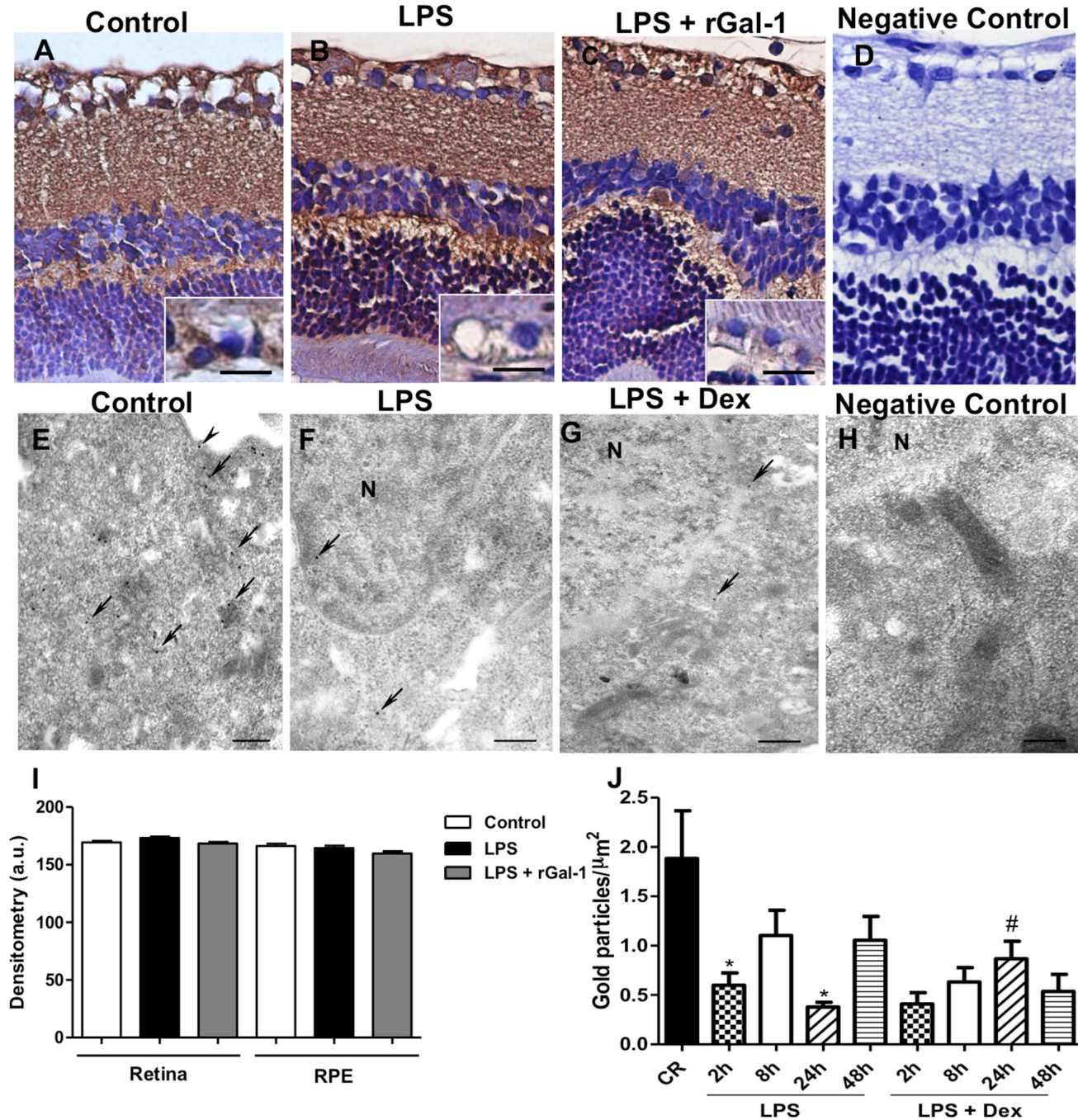
Figure 6. Gal-1 expression in the rat posterior eye segment and ARPE-19 cells. **A–C**: Similar immunostain for galectin-1 (Gal-1) in the retina was detected in the control, lipopolysaccharide (LPS) and LPS + recombinant Gal-1 (rGal-1) groups. Insets of figures A-C showed a detail of the RPE. **D**: No immunostaining was detected in the negative control section. Counterstain: hematoxylin. Bars: 20 µm. **E-G**: Immunogold electron micrograph on ARPE-19 cells under different conditions showing the localization of Gal-1 in the plasma membrane (arrowhead), cytosol, and nucleus (N; arrows). Strong immunoreactivity for Gal-1 in the control cells (**E**) is shown compared to LPS-stimulated cells at 24 h with or without dexamethasone (Dex) treatment (**F-G**). **H**: Absence of gold labeling in sections incubated with nonimmune goat anti-rabbit serum (negative control). Bars: 0.5 µm. **I**: Densitometric analysis of Gal-1 expression in the layers of the retina (plexiform and ganglion cells) and the RPE. Values (arbitrary units [a.u.]) are expressed as the mean ± SEM of Gal-1 immunoreactivity. **J**: Density of Gal-1 immunogold particles. Data are the mean ± SEM of gold particles per µm². *p<0.05 versus control; #p<0.05 versus LPS 24 h.

treated with rGal-1 (Figure 5G,H; p<0.001). There was no immunostaining in the eye used as negative control section (without primary antibody; Figure 5J). The data obtained through western blotting analysis confirmed the modulation of Gal-1 protein 24 h after LPS injection, due to an increase in its endogenous expression in supernatants of ocular tissues (Figure 5L; p<0.05).

The retinal layers showed immunostaining for Gal-1, mainly in the RPE, outer and inner plexiform strata, and ganglion cells of all studied groups (Figure 6A-C). Densitometry revealed a similar immunostaining pattern in these retinal layers among the control and LPS groups, indicating that this protein is a structural component of this region (Figure 6I). No immunostaining was detected in the ocular tissues used as negative control section (Figure 6D).

To correlate the in vivo findings with other quantitative assays, we determined the endogenous expression of Gal-1 in retinal pigment epithelial cells (ARPE-19 cells/RPE) via transmission electron microscopy. Gal-1 immunogold labeling was detected in the RPE in the plasma membrane, cytoplasm, and nucleus (Figure 6E-G). LPS-stimulated cells showed modest Gal-1 immunoreactivity in their subcellular compartments after 2 (p<0.05) and 24 h (Figure 6F; p<0.05) compared to the control group (Figure 6E). Dex treatment increased Gal-1 expression in these cells after 24 h (Figure 6G; p<0.05). These ultrastructural observations were confirmed by the data on the density of gold particles in these cells (Figure 6J). No labeling was detected in the negative control section (Figure 6H).

DISCUSSION

Despite advances in elucidating the role of Gal-1 in models of autoimmune diseases, its expression and effects on innate immune cells in ocular inflammatory processes have been poorly studied [18,23,39]. In this research, we developed in vivo and in vitro experimental models to evaluate different aspects of the actions of Gal-1 in the ocular tissues under inflammatory conditions.

Treatment with rGal-1 revealed the anti-inflammatory activities of this protein at 24 h through a decrease in the leukocyte influx into ocular tissues, AqH, and blood, as well as a reduction in the production of IL-1β and IL-6 in ocular tissues during EIU. The release of cytokines by activated inflammatory cells has been implicated in the pathogenesis of EIU. Among these cytokines, TNF-α, IL-1β, and IL-6 play an important role in the process of EIU [40], and they are produced by a wide variety of inflammatory cells, including neutrophils and mononuclear phagocytic cells [41,42], which are the main infiltrating cells in this inflammation [43]. These

findings are in line with in vivo tests showing that preadministration of Gal-1 inhibits the extravasation of neutrophils into the peritoneal cavity 4 h after the administration of carrageenan in rats [34] and IL-1β [30] and zymosan in mice [31]. In addition, the anti-migratory effect of this protein was shown to be associated with the inhibition of the release of the proinflammatory cytokines TNF-α and IL-1β but not that of IL-6 [31]. Thus, rGal-1 treatment ameliorates EIU manifestation by decreasing leukocyte migration and proinflammatory cytokine release in ocular tissues.

Supporting our in vivo data, rGal-1 also reduced the levels of IL-8 and IL-6 in LPS-stimulated ARPE-19 cells after 24 h, in comparison with untreated LPS-stimulated cells, through the negative regulation of COX-2 expression. It is well known that in several cell types, LPS is the major inducer of redox-sensitive transcription factor nuclear factor-κB (NF-κB), which plays a pivotal role in triggering an array of proinflammatory genes such as TNF-α, IL-1β, IL-6, IL-8, and COX-2 in inflammatory diseases, including endotoxin- and autoimmune-induced uveitis [3,44,45].

Our results obtained from flow cytometry corroborate the quantification of inflammatory cells, demonstrating a significant increase in the percentage of CD62L-positive cells 24 h after LPS injection. This confirmed the occurrence of cell activation caused by LPS. However, at the same experimental time point, treatment with rGal-1 increased the percentage of CD11b- and CD11b/CD62L-positive cells; moreover, in the 48 h LPS group (data not shown), a phase characterized by the diminished influx of leukocytes in this EIU model was obtained [3]. Interestingly, rGal-1 also increased the influx of mononuclear phagocytic cells in the AqH and blood at 24 h, which is consistent with high levels of adhesion molecules detected by immunoblot assays of rat ocular tissues. These results are consistent with in vitro assays demonstrating the role of Gal-1 in monocyte chemotaxis, induced by its carbohydrate-binding function (which was reduced by 65% in the presence of lactose) and the mitogen-activated protein kinase (MAPK) pathways [46]. In addition, the administration of exogenous Gal-1 appears to play a role in the activation of these cells, particularly in dendritic cells, by increasing the secretion of proinflammatory cytokines such as the chemokine MCP-1 [47]. Supporting this, our in vivo and in vitro data exhibited increased MCP-1 levels after treatment with rGal-1.

In a mouse model of zymosan-induced peritonitis, highly significant levels of CD11b expression were detected at 24 h by flow cytometry analysis in blood PMN from rGal-1 pretreated animals. However, this effect was not associated with an increase in cell transmigration on mesentery [31].

In vitro experiments using human neutrophils activated by platelet PAF showed that Gal-1 has no effect on the expression of CD62L and CD11b at low concentrations (~2.75 to 27.5 nM), but is capable of inhibiting the capture and rolling of these cells in the endothelium [48]. Nevertheless, at high concentrations (~275 nM), Gal-1 increases the adherence of neutrophils stimulated by PAF to the endothelium [48] and stimulates the chemotaxis of these cells [49]. In keeping with this, in our experimental model of uveitis, the inhibitory effect of Gal-1 on neutrophil recruitment may have occurred due to the low concentration of this lectin applied (3 µg/100 µl per animal), causing an imbalance in the expression of adhesion molecules and therefore negatively regulating cell transmigration at 24 h. Researchers have reported that Gal-1 inhibits IL-1β-induced recruitment of PMN leukocytes into the mouse peritoneal cavity, as well as their chemotaxis and transendothelial migration [30].

Following the detection of the anti-inflammatory action of exogenous Gal-1, western blotting analysis revealed upregulation of endogenous Gal-1 in the eyes 24 h after LPS injection, which was confirmed via immunohistochemistry analysis of the anterior segment. Gal-1 was expressed at particularly high levels in the epithelial cells of the cornea, conjunctiva, ciliary processes, and iris, as well as in endothelial cells. These results support the published finding that Gal-1 is expressed in the anterior segment of the human eye [50]. Modulation of this protein was also observed in a carrageenan-induced rat peritonitis model in which neutrophils showed low levels of endogenous Gal-1 during early acute inflammation (4 h) and high levels after 24 h [51]. In addition, pharmacological treatment with rGal-1 induced a decrease of its endogenous expression in the anterior eye segment, most likely as a negative feedback mechanism. In the posterior eye segment, Gal-1 expression was also observed in the retina in all experimental groups, specifically in the ganglion cells, the inner and outer plexiform layers and the PE, indicating a structural function for this protein in this tissue. Pharmacological treatment with rGal-1 produced no significant change in the endogenous protein levels in relation to the LPS group. Similarly, some studies have demonstrated Gal-1 expression in human, bovine, and rat retinas [52,53] and suggested that this protein functions in the accession of the photoreceptors and the outer plexiform layer through interaction with specific glycoconjugates [52]. Therefore, although Gal-1 can be considered a structural protein of the retina, it may also be secreted into the extracellular medium during the inflammatory process, indicating its anti-inflammatory action.

Based on the relevance of the phenotypic and functional characteristics of human ARPE-19 cells to inflammation [54] and to confirm the in vivo rodent data, we subsequently assessed Gal-1 expression in ARPE-19 cells activated by LPS and treated with rGal-1 by transmission electron microscopy. Gal-1 immunoreactivity was detected in the plasma membrane, cytosol, and nucleus under different conditions. The activation of cells using LPS decreased the endogenous levels of Gal-1 at 2 and 24 h, indicating the externalization of this protein during the inflammatory process and its participation in the physiology of control RPE cells. This result confirms that the expression of Gal-1 in RPE cells is positively modulated during the process of cell differentiation and proliferation, particularly under the effect of hepatic growth factor (HGF) [55]. In contrast, increased levels of Gal-1 protein expression were detected after Dex treatment (24 h) compared with untreated cells, suggesting a role of the endogenous glucocorticoid in the regulation of this protein in a temporal manner. Previous investigations using nasal polyps [56-58] also demonstrated the upregulation of Gal-1 mRNA and protein following treatment with budesonide and betamethasone glucocorticoids, particularly in epithelial and connective tissues.

Altogether, the in vivo and in vitro data showed that Gal-1 may represent a potential target for the treatment of inflammatory ocular conditions, especially uveitis. Future studies will address the molecular pathways involved in Gal-1 regulation of the inflammatory response.

APPENDIX 1. STR ANALYSIS OF ARPE 19 CELLS.

To access the data, click or select the words "Appendix 1."

REFERENCES

1. Rosenbaum JT, McDevitt HO, Guss RB, Egbert PR. Endotoxin-induced uveitis in rats as a model for human disease. Nature 1980; 286:611-3. [PMID: 7402339].

2. Chang JH, McCluskey P, Missotten T, Ferrante P, Jalaludin B, Lightman S. Use of ocular hypotensive prostaglandin analogues in patients with uveitis: does their use increase anterior uveitis and cystoid macular oedema? Br J Ophthalmol 2008; 92:916-21. [PMID: 18460537].

3. Girol AP, Mimura KK, Drewes CC, Bolonheis SM, Solito E, Farsky SH, Gil CD, Oliani SM. Anti-Inflammatory Mechanisms of the Annexin A1 Protein and Its Mimetic Peptide Ac2–26 in Models of Ocular Inflammation In Vivo and In Vitro. J Immunol 2013; 190:5689-701. [PMID: 23645879].

4. Ruiz-Moreno JM, Thillaye B, de Kozak Y. Retino-choroidal changes in endotoxin-induced uveitis in the rat. Ophthalmic Res 1992; 24:162-8. [PMID: 1407958].

5. Altan-Yaycioglu R, Akova YA, Akca S, Yilmaz G. Inflammation of the posterior uvea: findings on fundus fluorescein and indocyanine green angiography. Ocul Immunol Inflamm 2006; 14:171-9. [PMID: 16766401].

6. da Silva PS, Girol AP, Oliani SM. Mast cells modulate the inflammatory process in endotoxin-induced uveitis. Mol Vis 2011; 17:1310-9. [PMID: 21633711].

7. Chang JH, McCluskey PJ, Wakefield D. Toll-like receptors in ocular immunity and the immunopathogenesis of inflammatory eye disease. Br J Ophthalmol 2006; 90:103-8. [PMID: 16361678].

8. Goureau O, Bellot J, Thillaye B, Courtois Y, de Kozak Y. Increased nitric oxide production in endotoxin-induced uveitis. Reduction of uveitis by an inhibitor of nitric oxide synthase. J Immunol 1995; 154:6518-23. [PMID: 7539024].

9. Lennikov A, Kitaichi N, Noda K, Ando R, Dong Z, Fukuhara J, Kinoshita S, Namba K, Mizutani M, Fujikawa T, Itai A, Ohno S, Ishida S. Amelioration of endotoxin-induced uveitis treated with an IκB kinase β inhibitor in rats. Mol Vis 2012; 18:2586-97. [PMID: 23112571].

10. Medeiros R, Rodrigues GB, Figueiredo CP, Rodrigues EB, Grumman A, Menezes-de-Lima O, Passos GF, Calixto JB. Molecular mechanisms of topical anti-inflammatory effects of lipoxin A(4) in endotoxin-induced uveitis. Mol Pharmacol 2008; 74:154-61. [PMID: 18413658].

11. Li S, Lu H, Hu X, Chen W, Xu Y, Wang J. Expression of TLR4-MyD88 and NF-κB in the iris during endotoxin-induced uveitis. Mediators Inflamm 2010; xxx:748218-.

12. Kalariya NM, Reddy AB, Ansari NH, VanKuijk FJ, Ramana KV. Preventive effects of ethyl pyruvate on endotoxin-induced uveitis in rats. Invest Ophthalmol Vis Sci 2011; 52:5144-52. [PMID: 21551413].

13. Touchard E, Omri S, Naud MC, Berdugo M, Deloche C, Abadie C, Jonet L, Jeanny JC, Crisanti P, de Kozak Y, Combette JM, Behar-Cohen F. A peptide inhibitor of c-Jun N-terminal kinase for the treatment of endotoxin-induced uveitis. Invest Ophthalmol Vis Sci 2010; 51:4683-93. [PMID: 20393119].

14. Srivastava A, Rajappa M, Kaur J. Uveitis: Mechanisms and recent advances in therapy. Clin Chim Acta 2010; 411:1165-71. [PMID: 20416287].

15. Larson T, Nussenblatt RB, Sen HN. Emerging drugs for uveitis. Expert Opin Emerg Drugs 2011; 16:309-22. [PMID: 21210752].

16. Rosenbaum JT. Future for biological therapy for uveitis. Curr Opin Ophthalmol 2010; 21:473-7. [PMID: 20829688].

17. Perillo NL, Marcus ME, Baum LG. Galectins: versatile modulators of cell adhesion, cell proliferation, and cell death. J Mol Med (Berl) 1998; 76:402-12. [PMID: 9625297].

18. Rabinovich GA, Ariel A, Hershkoviz R, Hirabayashi J, Kasai KI, Lider O. Specific inhibition of T-cell adhesion to extracellular matrix and proinflammatory cytokine secretion by human recombinant galectin-1. Immunology 1999; 97:100-6. [PMID: 10447720].

19. Santucci L, Fiorucci S, Cammilleri F, Servillo G, Federici B, Morelli A. Galectin-1 exerts immunomodulatory and protective effects on concanavalin A-induced hepatitis in mice. Hepatology 2000; 31:399-406. [PMID: 10655263].

20. Cooper D, Ilarregui JM, Pesoa SA, Croci DO, Perretti M, Rabinovich GA. Multiple functional targets of the immunoregulatory activity of galectin-1: Control of immune cell trafficking, dendritic cell physiology, and T-cell fate. Methods Enzymol 2010; 480:199-244. [PMID: 20816212].

21. Cooper D, Iqbal AJ, Gittens BR, Cervone C, Perretti M. The effect of galectins on leukocyte trafficking in inflammation: sweet or sour? Ann N Y Acad Sci 2012; [PMID: 22256855].

22. Cooper DN, Barondes SH. God must love galectins; he made so many of them. Glycobiology 1999; 9:979-84. [PMID: 10521533].

23. Liu FT, Rabinovich GA. Galectins: regulators of acute and chronic inflammation. Ann N Y Acad Sci 2010; 1183:158-82. [PMID: 20146714].

24. Offner H, Celnik B, Bringman TS, Casentini-Borocz D, Nedwin GE, Vandenbark AA. Recombinant human beta-galactoside binding lectin suppresses clinical and histological signs of experimental autoimmune encephalomyelitis. J Neuroimmunol 1990; 28:177-84. [PMID: 1694534].

25. Rabinovich GA, Daly G, Dreja H, Tailor H, Riera CM, Hirabayashi J, Chernajovsky Y. Recombinant galectin-1 and its genetic delivery suppress collagen-induced arthritis via T cell apoptosis. J Exp Med 1999; 190:385-98. [PMID: 10430627].

26. Toscano MA, Commodaro AG, Ilarregui JM, Bianco GA, Liberman A, Serra HM, Hirabayashi J, Rizzo LV, Rabinovich GA. Galectin-1 suppresses autoimmune retinal disease by promoting concomitant Th2- and T regulatory-mediated anti-inflammatory responses. J Immunol 2006; 176:6323-32. [PMID: 16670344].

27. Perone MJ, Bertera S, Tawadrous ZS, Shufesky WJ, Piganelli JD, Baum LG, Trucco M, Morelli AE. Dendritic cells expressing transgenic galectin-1 delay onset of autoimmune diabetes in mice. J Immunol 2006; 177:5278-89. [PMID: 17015713].

28. Barondes SH, Cooper DN, Gitt MA, Leffler H. Galectins. Structure and function of a large family of animal lectins. J Biol Chem 1994; 269:20807-10. [PMID: 8063692].

29. Rabinovich GA, Sotomayor CE, Riera CM, Bianco I, Correa SG. Evidence of a role for galectin-1 in acute inflammation. Eur J Immunol 2000; 30:1331-9. [PMID: 10820379].

30. La M, Cao TV, Cerchiaro G, Chilton K, Hirabayashi J, Kasai K, Oliani SM, Chernajovsky Y, Perretti M. A novel biological

activity for galectin-1: inhibition of leukocyte-endothelial cell interactions in experimental inflammation. Am J Pathol 2003; 163:1505-15. [PMID: 14507657].

31. Gil CD, Gullo CE, Oliani SM. Effect of exogenous galectin-1 on leukocyte migration: modulation of cytokine levels and adhesion molecules. Int J Clin Exp Pathol 2010; 4:74-84. [PMID: 21228929].

32. Iqbal AJ, Sampaio AL, Maione F, Greco KV, Niki T, Hirashima M, Perretti M, Cooper D. Endogenous galectin-1 and acute inflammation: emerging notion of a galectin-9 pro-resolving effect. Am J Pathol 2011; 178:1201-9. [PMID: 21356371].

33. Seropian IM, Cerliani JP, Toldo S, Van Tassell BW, Ilarregui JM, González GE, Matoso M, Salloum FN, Melchior R, Gelpi RJ, Stupirski JC, Benatar A, Gómez KA, Morales C, Abbate A, Rabinovich GA. Galectin-1 controls cardiac inflammation and ventricular remodeling during acute myocardial infarction. Am J Pathol 2013; 182:29-40. [PMID: 23142379].

34. Gil CD, Cooper D, Rosignoli G, Perretti M, Oliani SM. Inflammation-induced modulation of cellular galectin-1 and −3 expression in a model of rat peritonitis. Inflamm Res 2006; 55:99-107. [PMID: 16673152].

35. Oliani SM, Perretti M. Cell localization of the anti-inflammatory protein annexin 1 during experimental inflammatory response. Ital J Anat Embryol 2001; 106:Suppl 169-77. [PMID: 11729999].

36. Dunn KC, Aotaki-Keen AE, Putkey FR, Hjelmeland LM. ARPE-19, a human retinal pigment epithelial cell line with differentiated properties. Exp Eye Res 1996; 62:155-69. [PMID: 8698076].

37. Chang SW, Chou SF, Yu SY. Dexamethasone reduces mitomycin C-related inflammatory cytokine expression without inducing further cell death in corneal fibroblasts. Wound Repair Regen 2010; 18:59-69. [PMID: 20002897].

38. Leung KW, Barnstable CJ, Tombran-Tink J. Bacterial endotoxin activates retinal pigment epithelial cells and induces their degeneration through IL-6 and IL-8 autocrine signaling. Mol Immunol 2009; 46:1374-86. [PMID: 19157552].

39. Mochizuki M, Sugita S, Kamoi K. Immunological homeostasis of the eye. Prog Retin Eye Res 2013; 33:10-27. [PMID: 23108335].

40. Zheng C, Lei C, Chen Z, Zheng S, Yang H, Qiu Y, Lei B. Topical administration of diminazene aceturate decreases inflammation in endotoxin-induced uveitis. Mol Vis 2015; 21:403-11. [PMID: 25883526].

41. Yang S, Lu H, Wang J, Qi X, Liu X, Zhang X. The effect of toll-like receptor 4 on macrophage cytokines during endotoxin induced uveitis. Int J Mol Sci 2012; 13:7508-20. [PMID: 22837708].

42. Akira S, Hirano T, Taga T, Kishimoto T. Biology of multifunctional cytokines: IL 6 and related molecules (IL 1 and TNF). FASEB J 1990; 4:2860-7. [PMID: 2199284].

43. McMenamin PG, Crewe J. Endotoxin-induced uveitis. Kinetics and phenotype of the inflammatory cell infiltrate and the response of the resident tissue macrophages and dendritic cells in the iris and ciliary body. Invest Ophthalmol Vis Sci 1995; 36:1949-59. [PMID: 7657537].

44. Srivastava SK, Ramana KV. Focus on molecules: nuclear factor-kappaB. Exp Eye Res 2009; 88:2-3. [PMID: 18472097].

45. Tak PP, Firestein GS. NF-kappaB: a key role in inflammatory diseases. J Clin Invest 2001; 107:7-11. [PMID: 11134171].

46. Malik RK, Ghurye RR, Lawrence-Watt DJ, Stewart HJ. Galectin-1 stimulates monocyte chemotaxis via the p44/42 MAP kinase pathway and a pertussis toxin-sensitive pathway. Glycobiology 2009; 19:1402-7. [PMID: 19561030].

47. Fulcher JA, Hashimi ST, Levroney EL, Pang M, Gurney KB, Baum LG, Lee B. Galectin-1-matured human monocyte-derived dendritic cells have enhanced migration through extracellular matrix. J Immunol 2006; 177:216-26. [PMID: 16785517].

48. Cooper D, Norling LV, Perretti M. Novel insights into the inhibitory effects of Galectin-1 on neutrophil recruitment under flow. J Leukoc Biol 2008; 83:1459-66. [PMID: 18372340].

49. Auvynet C, Moreno S, Melchy E, Coronado-Martínez I, Montiel JL, Aguilar-Delfín I, Rosenstein Y. Galectin-1 promotes human neutrophil migration. Glycobiology 2013; 23:32-42. [PMID: 22942212].

50. Fautsch MP, Silva AO, Johnson DH. Carbohydrate binding proteins galectin-1 and galectin-3 in human trabecular meshwork. Exp Eye Res 2003; 77:11-6. [PMID: 12823983].

51. Gil CD, La M, Perretti M, Oliani SM. Interaction of human neutrophils with endothelial cells regulates the expression of endogenous proteins annexin 1, galectin-1 and galectin-3. Cell Biol Int 2006; 30:338-44. [PMID: 16530434].

52. Uehara F, Ohba N, Ozawa M. Isolation and characterization of galectins in the mammalian retina. Invest Ophthalmol Vis Sci 2001; 42:2164-72. [PMID: 11527926].

53. Romero MD, Muiño JC, Bianco GA, Ferrero M, Juarez CP, Luna JD, Rabinovich GA. Circulating anti-galectin-1 antibodies are associated with the severity of ocular disease in autoimmune and infectious uveitis. Invest Ophthalmol Vis Sci 2006; 47:1550-6. [PMID: 16565391].

54. Paimela T, Ryhänen T, Mannermaa E, Ojala J, Kalesnykas G, Salminen A, Kaarniranta K. The effect of 17beta-estradiol on IL-6 secretion and NF-kappaB DNA-binding activity in human retinal pigment epithelial cells. Immunol Lett 2007; 110:139-44. [PMID: 17532054].

55. Alge CS, Priglinger SG, Kook D, Schmid H, Haritoglou C, Welge-Lussen U, Kampik A. Galectin-1 influences migration of retinal pigment epithelial cells. Invest Ophthalmol Vis Sci 2006; 47:415-26. [PMID: 16384992].

56. Delbrouck C, Doyen I, Belot N, Decaestecker C, Ghanooni R, de Lavareille A, Kaltner H, Choufani G, Danguy A, Vandenhoven G, Gabius HJ, Hassid S, Kiss R. Galectin-1 is overexpressed in nasal polyps under budesonide and inhibits eosinophil migration. Lab Invest 2002; 82:147-58. [PMID: 11850528].

57. Sena AA, Provazzi PJ, Fernandes AM, Cury PM, Rahal P, Oliani SM. Spatial expression of two anti-inflammatory mediators, annexin 1 and galectin-1, in nasal polyposis. Clin Exp Allergy 2006; 36:1260-7. [PMID: 17014434].

58. Fernandes AM, Babeto E, Rahal P, Provazzi PJ, Hidalgo CA, Anselmo-Lima WT. Expression of genes that encode the annexin-1 and galectin-1 proteins in nasal polyposis and their modulation by glucocorticoid. Braz J Otorhinolaryngol 2010; 76:213-8. [PMID: 20549082].